26th ABCM International Congress of Mechanical Engineering
November 22-26, 2021. Florianópolis, SC, Brazil

COB-2021-0004
Numerical study of a ferrofluid flow in a T-junction

Hugo Marmori de Morais
School of Mechanical Engineering, University of Campinas, Campinas-SP 13083 860, Brazil
hugo.marmori@gmail.com
Adriano Possebon Rosa
Mechanical Engineering Department, University of Brasilia, Brasilia-DF 70910 900, Brazil
aprosa@unb.br

Abstract. *The main objective of the present study is to investigate the modifications on the ferrofluid flow in a T-junction caused by an external magnetic field. The authors developed a FORTRAN 95 software to simulate the flow of Newtonian fluids and ferrofluids within a T-junction, using the staggered grid, finite differences, and the second-order projection method. They used different combinations of the magnetic number and the Reynolds number to analyze the flow in geometry with fixed dimensions. The simulations were conducted until they reached the steady-state, at which point the outflow rates cease to vary. The results obtained for the ferrofluid were compared with the data for Newtonian fluids. Without the application of the magnetic field, it is harder for the fluid to go through the perpendicular outlet as the number of Reynolds increases, due to the fluid inertia. The application of the magnetic field and consequently the increase in the Magnetic number implies a greater tendency of the fluid to follow the field direction, which allows for eventual control of the fluid. However, the results show that it is not possible to remove the vortex present in a usual T-junction flow.*

Keywords: *Ferrofluid, T-junction, Projection Method, Finite Differences, CFD.*

1. INTRODUCTION

Ferrofluids are stable colloidal suspensions of magnetic nanoparticles in a Newtonian fluid (Rosensweig, 2013). The particles are usually made os Niquel, Cobalt and Iron and they are covered by a surfactant layer in order to prevent aggregation. They do not transmit electricity, but they are affected by a magnetic field. It is possible to change its flow or to increase its viscosity according to the applied magnetic field. Engineers use this kind of fluid in a variety of applications. For example, ferrofluids are used in Hard Drives as a sealing material, preventing dust from damaging the system. Ferrofluids can be found as well in sound speakers because of their capability to transfer heat and to dump vibrations (Raj *et al.*, 1995).

They are used in medicine, such as Magnetic Drug Targeting (MDT) where drugs are guided by magnetic fields to specific locations in the body (Ganguly *et al.*, 2005). Also, there is magnetohyperthemia, which is used in cancer treatment. An alternative magnetic field is applied and, due to its magnetic properties, the ferrofluid temperature increases, which makes tumor cell weaker and increase the efficiency of chemotherapy (Hiergeist *et al.*, 1999).

A T-junction is a component with three openings, two exits, and one entrance, or two entrances, and one exit. It is present in hydraulic installations, air conditioning systems, blood vessels, etc. It is used to separate multiphase flow (Azzopardi and Whalley, 1982). It is a common connection that have well known pressure drop coefficient (White, 2010). Much has been studied in an experimental way the capacity of this configuration to form bubbles and drops in multiphase flows (Garstecki *et al.*, 2006), including with ferrofluid emulsion (Tan and Nguyen, 2011), due to the shape of its geometry that allows this phenomenon.

Previous studies were concerned with pressure loss for a Newtonian fluid, either in the main or in the secondary branch. Recent studies evaluated viscoelastic fluids in transient (Matos and Oliveira, 2014) or permanent flow (Matos and Oliveira, 2013). And Gerdroodbary *et al.* (2018) analyzed the increase in heat transfer at a T-junction using a ferrofluid.

The main goal of this work is to investigate the influence of a magnetic field over a ferrofluid inside a T-junction. The authors want to change the flow and the flow rate through each exit of a T-junction. The analysis is conducted numerically using a software developed by the authors.

2. GOVERNING EQUATIONS

For an incompressible flow, the continuity equation is

$$\nabla \cdot \mathbf{u} = 0, \tag{1}$$

where $\mathbf{u}$ is the velocity vector (Batchelor, 2000). Cauchy equation is used to describe any continuum material movement

(Chandrasekharaiah and Debnath, 2014), it is written as

$$\rho\frac{D\mathbf{u}}{Dt} = \nabla\cdot\mathbf{T} + \rho\mathbf{f}, \tag{2}$$

where ρ is the density, t is the time, $\mathbf{T}$ is the stress tensor and $\mathbf{f}$ is a vector representing force field, and the operator $\frac{D}{Dt}$ is the material derivative. What makes a Newtonian fluid different of a ferrofluid is the stress tensor. For a Newtonian fluid, $\mathbf{T}$ is

$$\mathbf{T}_n = -P\mathbf{I} + \mu\left(\nabla\mathbf{u} + (\nabla\mathbf{u})^T\right), \tag{3}$$

where $\mathbf{T}_n$ is the Newtonian stress tensor, P is the pressure field, $\mathbf{I}$ is the identity tensor, μ is the dynamic viscosity (Aris, 2012). For a symmetric ferrofluid, there is one more term related to magnetic forces, so equation 3 becomes

$$\mathbf{T}_f = -P\mathbf{I} + \mu(\nabla\mathbf{u} + (\nabla\mathbf{u})^T) - \frac{1}{2}\mu_0(\mathbf{H}\cdot\mathbf{H})\mathbf{I} + \mathbf{BH}. \tag{4}$$

The new variables are the magnetic field, $\mathbf{H}$, and the inductive magnetic field $\mathbf{B}$. The constant μ_0 is the permeability of a magnetic field in vaccum. $\mathbf{B}$ and $\mathbf{H}$ are related by

$$\mathbf{B} = \mu_0(\mathbf{H} + \mathbf{M}), \tag{5}$$

$\mathbf{M}$ consist on the magnetization, which is the volumetric mean of the dipole moments of all particles present in the fluid (Rosensweig, 2013).

The substitution of equations 3, 4 into equatino 2 results in the moment balance for a Newtonian fluid,

$$\rho\frac{D\mathbf{u}}{Dt} = -\nabla P + \mu\nabla^2\mathbf{u} + \rho\mathbf{f}, \tag{6}$$

and a ferrofluid,

$$\rho\frac{D\mathbf{u}}{Dt} = -\nabla P + \mu\nabla^2\mathbf{u} + \mu_0\mathbf{M}\cdot\nabla\mathbf{H} + \rho\mathbf{f}, \tag{7}$$

respectively. Equation 6 is known as the Navier-Stokes equation and equation 7 is known as the modified Navier-Stokes equation. The part of the equation that differs equations 6 and 7 is the Kelvin force, which happens due to the magnetization of the fluid and the gradient of the magnetic field (Rosensweig, 2013).

For a symmetric superparamagnetic ferrofluid, the magnetization vector aligns instantly to the magnetic field and there is no interference of the flow on the alignment. So it is not necessary to use an evolution magnetization model to describe the magnetization, which is given as

$$\mathbf{M} = \phi_m M_d L(\alpha_m)\hat{\mathbf{H}}, \tag{8}$$

where ϕ_m is the ratio between the volume of particles and the volume of the fluid, M_d is the solid magnetization, α_m is the ratio between the magnetic energy and the thermal energy, $L(\alpha_m)$ is the Langevin function, and $\hat{\mathbf{H}}$ is the unitary vector representing the direction of the magnetic field (Rosensweig, 2013). The Langevin function is

$$L(\alpha_m) = coth(\alpha_m) - \frac{1}{\alpha_m} \tag{9}$$

and α_m is

$$\alpha_m = \frac{\pi\mu_0 M_d H d_m^3}{6k_b T}, \tag{10}$$

where $coth$ represents the hyperbolic cotangent function, H is the modulus of the magnetic field, d_m is the diameter of the magnetic particle, k_b is the Boltzmann constant, and T is temperature.

The temperature has an important role in magnetization and, consequently, the Kelvin force will vary according to temperature. If the temperature increases, the Kelvin force will get smaller. And, for a symmetric superparamagnetic fluid, without a temperature gradient, the magnetic force will not affect ferrofluid flow. The temperature equation is given by

$$\frac{DT}{Dt} = \alpha_T\nabla^2 T, \tag{11}$$

where α_T is the thermal diffusivity (Cengel and Ghajar, 2009). The heat generated by the viscosity forces and the magnetic forces can be neglected because they are very small in comparison to the diffusion of temperature.

The governing equations are made non-dimensional by using the following variables (Batchelor, 2000):

$$t' = t\frac{U}{L}, \tag{12}$$

$$\mathbf{u}' = \frac{\mathbf{u}}{U}, \tag{13}$$

$$\mathbf{x}' = \frac{\mathbf{x}}{L}, \tag{14}$$

$$P' = \frac{P - P_0}{\rho U^2}. \tag{15}$$

$$\mathbf{H}' = \frac{\mathbf{H}}{H_0} \tag{16}$$

and

$$\mathbf{M}' = \frac{\mathbf{M}}{\phi_m M_d}. \tag{17}$$

U is the velocity reference and represents the average velocity in the inlet; L is the length reference, it represents the width between the T-junction walls; P_0 is the pressure reference; H_0 is the reference for the magnetic field, it represents the biggest value that H can achieve. The apostrophes represent that a variable is dimensionless. For temperature, it is used the difference between the hottest temperature and the colder temperature, so

$$\theta = \frac{T - T_c}{T_h - T_c}, \tag{18}$$

where θ is the dimensionless temperature difference, T_c is the coldest temperature, and T_h the hottest temperature. Using equations 12, 13, 14, 15, 16, 17, and 18, the gorverning equations in its dimensionless form become

$$\frac{D\mathbf{u}'}{Dt'} = -\nabla P' + \frac{1}{Re}\nabla^2\mathbf{u}' + Mn(\mathbf{M}' \cdot \nabla)\mathbf{H}', \tag{19}$$

$$\frac{D\theta}{Dt'} = \frac{1}{RePr}\nabla^2\theta \tag{20}$$

and

$$\mathbf{M}' = L(\alpha_m)\hat{\mathbf{H}}. \tag{21}$$

During the process to get dimensionless equations some number appear, they are the Reynolds number,

$$Re = \frac{\rho U L}{\mu}, \tag{22}$$

the Prandtl number,

$$Pr = \frac{\nu}{\alpha_T}, \tag{23}$$

and the magnetic number

$$Mn = \frac{\mu_0 \phi_m H_0 M_d}{\rho U^2}, \tag{24}$$

Each number represents a ratio between phenomenona that affects ferrofluid flow or Newtonian fluid flow. The Reynolds number, Re, represents the ratio between the inertial force and the viscosity force. The higher the Reynolds number, the more difficult is for the fluid to change direction or to diffuse its momentum (Milne-Thomson, 1996). The Prandtl Number, Pr, represents the ratio between momentum diffusion and thermal diffusion (Cengel and Ghajar, 2009). The last number presented is the magnetic number, Mn, which is the ratio between the magnetic forces and the inertial forces (Gerdroodbary *et al.*, 2018), if Mn is equal to zero, equation 19 become the dimensionless Navier-Stokes equation.

There is an implication, that the variable α_m is composed of a ratio with the temperature in the denominator. It is not possible to directly use the temperature based on its difference, as a division by zero would occur. Therefore, the simulation temperatures have been specified so that they are inserted in α_m. So the α_m is worked as follows, in this study,

$$\alpha_m = \frac{\alpha_0 H'}{1 + \frac{\theta \Delta T}{T_c}}. \tag{25}$$

H' is the intensity of the field in the dimensionless form, ΔT the temperature difference and T_c the cold temperature. The parameter α_0 is an auxiliary constant referring to the value of α_m can reach, it receives all other variables that are not shown in the equation 25, therefore

$$\alpha_0 = \frac{\pi \mu_0 M_d H_0 d_m^3}{6 k_b T_f}. \tag{26}$$

The choosen magnetic fields for this study are given by the following equations:

$$\mathbf{H}_1 = \frac{y}{l_y}\hat{\mathbf{e}}_y \tag{27}$$

and

$$\mathbf{H}_2 = -1 + \frac{y}{l_y}\hat{\mathbf{e}}_y. \tag{28}$$

They are simplifications of real magnetic fields, they were used because of its direct influence in the velocity field, $\mathbf{H}_1$ will move the fluid towards outlet 3 and $\mathbf{H}_2$ will move the flow towards outlet 2.

From this point and beyond, all variables are dimensionless, except when it is specified the dimension.

3. NUMERICAL METHOD

The partial differential equations 19 and 20 are solved numerically, using the finite difference method, both convective and diffusive terms were approximated by centered difference. It was used the second order projection method presented by Brown *et al.* (2001). This second order projection method uses a auxiliary variable ϕ which update the pressure and is calculated from the intermediate velocity vector $\mathbf{u}^*$, so the system of equations become

$$\frac{\mathbf{u}^* - \mathbf{u}^n}{\Delta t} + \mathbf{u}^{n+1/2} \cdot \nabla \mathbf{u}^{n+1/2}, = \frac{1}{2Re}\nabla^2(\mathbf{u}^* - \mathbf{u}^n) - \nabla P^{n-1/2} + Mn\mathbf{M}^{n+1/2} \cdot \nabla \mathbf{H}^{n+1/2}, \tag{29}$$

$$\frac{\nabla \cdot \mathbf{u}^*}{\Delta t} = \nabla^2 \phi^{n+1}, \tag{30}$$

$$\mathbf{u}^{n+1} = \mathbf{u}^* - \Delta t \nabla \phi^{n+1} \tag{31}$$

and

$$P^{n+1/2} = P^{n-1/2} + \phi^{n+1} - \frac{1}{2Re}\nabla^2 \phi^{n+1}. \tag{32}$$

The n index represents steps in time. For values calculated in $n + 1/2$, it was used the Adam-Bashforth interpolation.

It was used a staggered grid, in which velocity and pressure are evaluated at different points (Hirsch, 2007).

The CFL condition was used to prevent the simulation from diverging. This condition states that the flow advance in time must be less than the advance in space, so

$$Co = \frac{u \Delta t}{\Delta x} \tag{33}$$

where Co is the Courant Number (Hirsch, 2007), usually $Co = 1$.

3.1 MESH CONVERGENCE

The convergence study was done in a proper T-junction as shown in Figure 1. This connection component presents one entrance and two exits The flow enters the domain at inlet 1 fully developed and with pressure gradient equals to 0 at a flow rate of 1, and exits through both exits 2 and 3, also, fully developed. Both outlets have a pressure defined as 0 and a velocity gradient null. Dimension $L1$ is the length of the entrance, dimension $L2$ is the length of the main exit, first exit, or east exit, dimension $L3$ is the length of the auxiliary exit, second exit, or south exit. Dimensions $D1$ and $D2$ represent the distance between each wall channel. The fluid enters the domain completely developed, so $L1$ does not need to be similar to $L2$ and $L3$. $L2$ and $L3$ are of equal size, so the ratio of the length of the channels does not affect the flow. The dimensions used in the mesh convergence are shown at Table 1 In the convergence study, it was used four meshes: 800 nodes for $\Delta x = \Delta y = 0.2$, 3200 nodes for $\Delta x = \Delta y = 0.1$, 12800 nodes for $\Delta x = \Delta y = 0.05$ and 51200 nodes for $\Delta x = \Delta y = 0.025$. It was used three different ratios between Δt and Δx: 0.2, 0.1, 0.05. The simulations were conducted until time 10 was achieved. The Reynolds numbers evaluated were 20 and 100. The parameter for convergence is the flow rate at exit 3 or south exit.

Tables 2 through 7 show the results for the mesh convergence, where N_x is the number of nodes in x direction, N_y is the number of nodes in y direction, and Q_3 is the flow rate through outlet three. For a Reynolds of 20, the flow converged well in space. However, it is worth noting the disparity between the flow data for each step in time, from the largest to the smallest advance in time, there was a variation of up to 25.6%, this value is greater for $Re = 100$. Due to the results presented, the chosen mesh have 12800 nodes, and a Δt and Δx ratio of 0.1 .

Table 1. Dimension data for the simulations

Dimension	Length
D1	1
D2	1
L1	4
L2	15
L3	15

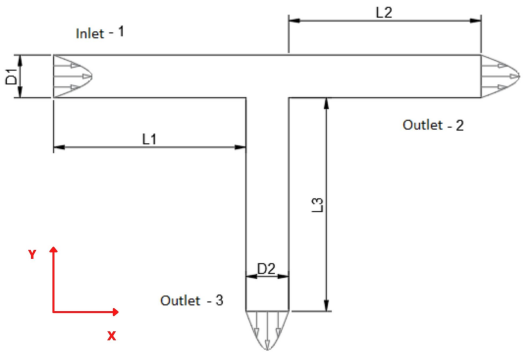

Figure 1. Schematic diagram of the T-junction used in this study

Table 2. Mesh convergence data for $t = 10$, $Re = 20$, Newtonian fluid, $\Delta t/\Delta x = 0.2$

Δx	Q_3
0.2	0.3789
0.1	0.3824
0.05	0.3820

Table 3. Mesh convergence data for: $t = 10$, $Re = 20$ e Newtonian fluid, $\Delta t/\Delta x = 0.1$

Δx	Q_3
0.2	0.4253
0.1	0.4558
0.05	0.4618

Table 4. Mesh convegence data for $t = 10$, $Re = 20$, Newtonian fluid, $\Delta t/\Delta x = 0.05$

Δx	Q_3
0.2	0.4378
0.1	0.4737
0.05	0.4798

Table 5. Mesh convergence data for $t = 10$, $Re = 100$, Newtonian fluid, $\Delta t/\Delta x = 0.2$

Δx	Q_3
0.1	0.6381
0.05	0.5578
0.025	0.5582

Table 6. Mesh convergence data for $t = 10$, $Re = 100$, Newtonian fluid, $\Delta t/\Delta x = 0.1$

Δx	Q_3
0.1	0.2080
0.05	0.1980
0.025	0.2004

Table 7. Mesh convergence data for $t = 10$, $Re = 100$ e fluido Newtoniano, $\Delta t/\Delta x = 0.05$

Δx	Q_3
0.1	0.2620
0.05	0.2499
0.025	0.2382

3.2 VALIDATION

To evaluate the program in the T configuration, the results were compared with the data obtained by Hayes *et al.* (1989). However, these authors used a domain, with different dimensions and calculating the Reynolds number based on the speed at the center of the parabola at the entrance. The dimensions used in the domain are shown in Table 8.

Table 8. Domain dimensions used by Hayes *et al.* (1989)

Dimension	Length
L1	2
L2	3
L3	3
D1	1
D2	1

Making the necessary changes and using a 120×80 mesh - with these nodes, the value of Δx and Δy determined in the mesh convergence is maintained - and a step in time of 0.005, up to t = 100, when the flow is permanent. The results are presented in Figure 2, where Q_2 is the flow rate through outlet 2. The results obtained in the software developed for this study are similar to those presented by Hayes *et al.* (1989) who obtained these data solving the streamline function by using the finite element method. There are tiny variations between the article in question and this work, but the results and the tendency remains similar.

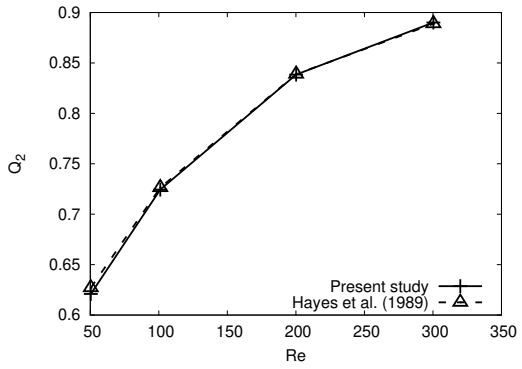

Figure 2. Flow rate through Q_2 according to the Reynolds number

4. RESULTS

For the analysis, the dimensions used are the ones in Table 1. The data for the simulations with the ferrofluid are shown in Table 9. The ferrofluid entered the geometry at temperature T_c and were heated by the walls at the entrance, until it gets right before the division of the T-junction, all the other walls are at temperature T_c. To guarantee that the flow is permanent at the ferrofluid case, the magnetic field switched on only at $t = 100$, then the simulation was conducted until $t = 200$.

Table 9. Temperature and magnetism data

Constant	Value
T_c, K	300
ΔT, K	100
α_0	1

4.1 PERMANENT FLOW

In figures 3 and 4, the typical flow velocity field at a T-junction with $Re = 100$ is shown. In these figures, the color variation corresponds to the velocity vector module. This flow is characterized by the formation of a large recirculation zone at the secondary branch because the fluid is unable to fully diffuse to the second arm due to its inertia (Hayes *et al.*, 1989). It also evidences the shock of the fluid with the corner of the domain. In figure 3, there is evidence that the fluid does not divide equally.

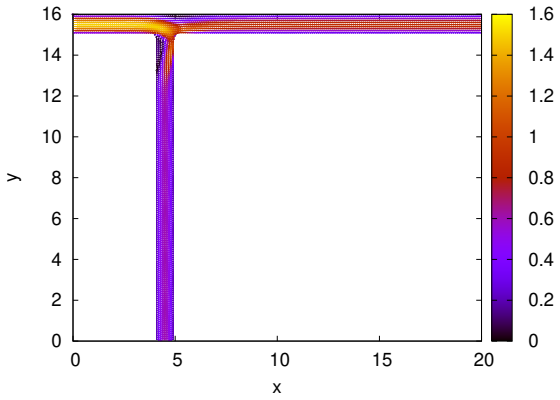

Figure 3. Velocity field for a ferrofluid, $t = 100$, $Re = 100$, $Mn = 0$, color represents the velocity vector modulus

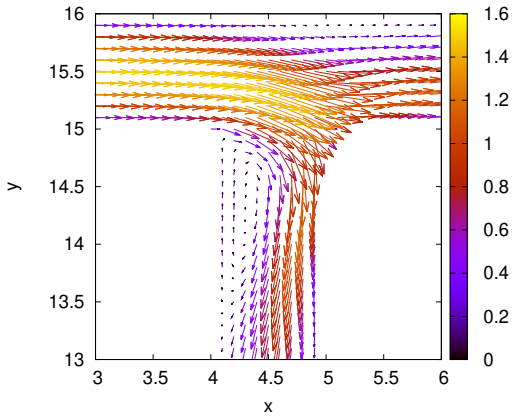

Figure 4. Velocity field for a ferrofluid, $t = 100$, $Re = 100$, $Mn = 0$, centered in the division, color represents the velocity vector modulus

Figures 5 and 6 show the velocity field for a ferrofluid flow with the magnetic field $\mathbf{H}_1$ applied. The presence of this magnetic field forces the ferrofluid to go through the south outlet. Most part of the fluid can not resist the magnetic forces, besides the high inertia. There is almost no fluid going to the east outlet, as can be seen by the dark colors of the velocity vectors. The detachment, that occurred without the magnetic field, is still present and it is responsible for the increase of the fluid velocity, which almost reaches 2. A second vortex appears at the main branch as a consequence of the low quantity of fluid in that region.

The last permanent flow analyzed is the one with the magnetic field $\mathbf{H}_2$ applied. This magnetic field forces the fluid to stay on the main branch and to go through outlet 2. The velocity field is shown at Figures 7 and 8. They show that the fluid almost stays untouched like there was no possible way to go down. The color scheme reinforces this idea as it is all dark in the secondary branch. A closer look reveals that there is a small percentage of fluid going in the south direction and that there is a recirculation zone like in the other cases.

4.2 FLOW RATE

The last analysis in this paper is concerned with the flow rate that goes out through each exit. Figure 9 shows that increasing the Reynolds number decreases the quantity of flow through exit 3. The bigger the inertia, the harder for the fluid to diffuse through the geometry as it was shown. This quantity of fluid going out has a limit because it can not have an exit with a flow rate bigger than 1. Looking to the ferrofluid case for $Re = 100$, the quantity of fluid that exits through

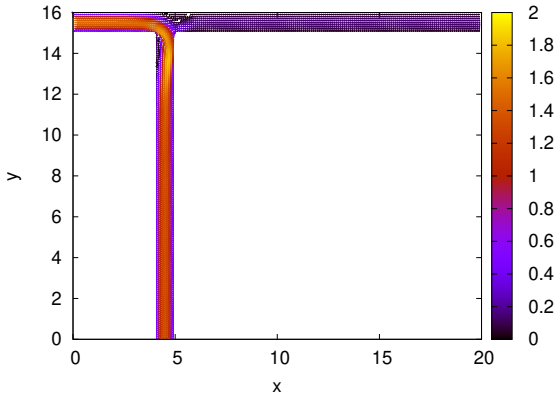

Figure 5. Velocity field for a Ferrofluid, $t = 100$, $Re = 100$, $Mn = 14$, magnetic field $\mathbf{H}_1$, color represents the velocity vector modulus

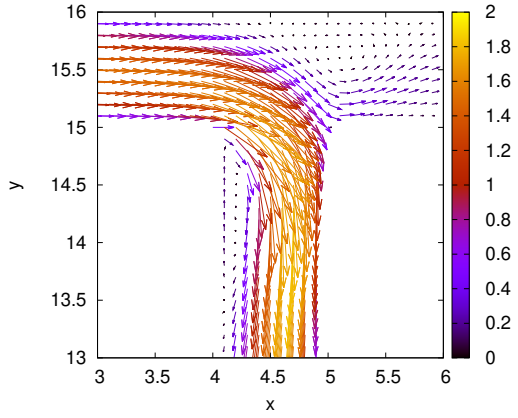

Figure 6. Velocity field for a Ferrofluid, $t = 100$, $Re = 100$, $Mn = 14$, magnetic field $\mathbf{H}_1$, centered in the division, color represents the velocity vector modulus

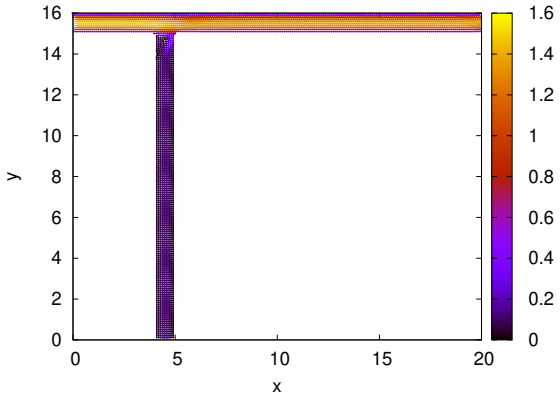

Figure 7. Velocity field for a Ferrofluid, $t = 100$, $Re = 100$, $Mn = 10$, magnetic field $\mathbf{H}_2$, color represents the velocity vector modulus

outlet 3 increases with the Magnetic Number for the magnetic field $\mathbf{H}_1$. The opposite occurs for the magnetic field $\mathbf{H}_2$, the bigger the magnetic number, the smaller the flow rate through exit 3. For $\mathbf{H}_1$ there is a point of change between the flow rates, and it is located near $Mn = 3$. For the magnetic field $\mathbf{H}_1$, it was necessary a bigger value of the magnetic number to achieve the same amount of flow rate than with $\mathbf{H}_2$, but inverted. This happens because $\mathbf{H}_2$ contribute for a natural tendency of the fluid to stay in the main axis due to its inertia. In both cases with $\mathbf{H}_1$ and $\mathbf{H}_2$ the flow rate varied almost linearly. This increase in the flow rate in ferrofluid case is due to the magnetic forces becoming predominant over the fluid, which is represented by the Magnetic Number, so the Kelvin force overcomes the inertia forces.

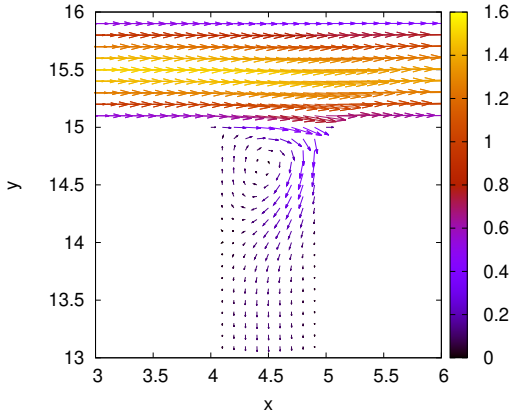

Figure 8. Velocity field for a Ferrofluid, $t = 100$, $Re = 100$, $Mn = 10$, magnetic field $\mathbf{H}_2$, centered in the division, color represents the velocity vector modulus

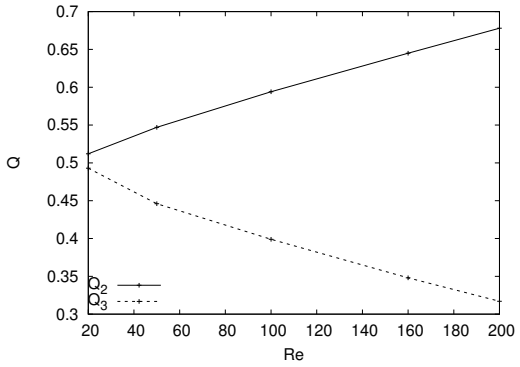

Figure 9. Flow rate for a Newtonian fluid according to the Reynolds number

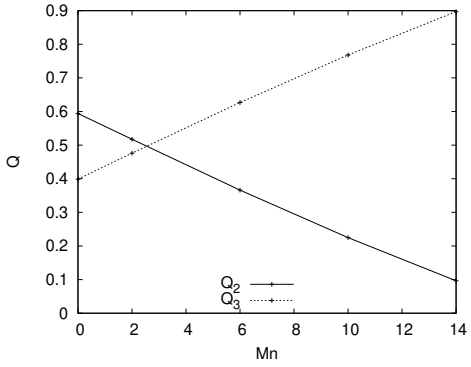

Figure 10. Flow rate for a ferrofluid with $Re = 100$ and magnetic field $\mathbf{H}_1$ according to the Magnetic number

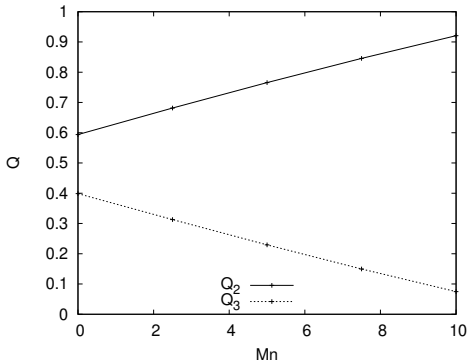

Figure 11. Flow rate for a ferrofluid with $Re = 100$ and magnetic field $\mathbf{H}_2$ according to the Magnetic number

5. CONCLUSION

This study presented the effect of a magnetic field applied to a ferrofluid inside a T-junction by using a CFD software developed by the authors. The presence of a magnetic field can change the behavior of a ferrofluid but it depends on its intensity related to the magnetic number. When a magnetic field similar to $\mathbf{H}_1$ is applied, the fluid tends to go down, and when $\mathbf{H}_2$ is applied it tends to keep flowing in the main channel. Some T-junction flow constructions were not removed by the magnetic field, like the vortex at the beginning of the second branch. Further studies can be done using a 3D geometry, an asymmetric ferrofluid, and the implementation of more realistic magnetic fields.

6. REFERENCES

Aris, R., 2012. *Vectors, tensors and the basic equations of fluid mechanics*. Courier Corporation.

Azzopardi, B.t. and Whalley, P., 1982. "The effect of flow patterns on two-phase flow in a T-junction". *International Journal of Multiphase Flow*, Vol. 8, No. 5, pp. 491–507.

Batchelor, G.K., 2000. *An introduction to fluid dynamics*. Cambridge university press.

Brown, D.L., Cortez, R. and Minion, M.L., 2001. "Accurate projection methods for the incompressible Navier-Stokes equations". *Journal of Computational Physics*, Vol. 168, No. 2, pp. 464–499.

Cengel, Y.A. and Ghajar, A.J., 2009. *Tranferência de Calor e Massa*. AMGH Editora.

Chandrasekharaiah, D. and Debnath, L., 2014. *Continuum mechanics*. Elsevier.

Ganguly, R., Gaind, A.P., Sen, S. and Puri, I.K., 2005. "Analyzing ferrofluid transport for magnetic drug targeting". *Journal of Magnetism and Magnetic Materials*, Vol. 289, pp. 331–334.

Garstecki, P., Fuerstman, M.J., Stone, H.A. and Whitesides, G.M., 2006. "Formation of droplets and bubbles in a microfluidic T-junction—scaling and mechanism of break-up". *Lab on a Chip*, Vol. 6, No. 3, pp. 437–446.

Gerdroodbary, M.B., Sheikholeslami, M., Mousavi, S.V., Anazadehsayed, A. and Moradi, R., 2018. "The influence of non-uniform magnetic field on heat transfer intensification of ferrofluid inside a T-junction". *Chemical Engineering and Processing-Process Intensification*, Vol. 123, pp. 58–66.

Hayes, R., Nandakumar, K. and Nasr-El-Din, H., 1989. "Steady laminar flow in a 90 degree planar branch". *Computers & Fluids*, Vol. 17, No. 4, pp. 537–553.

Hiergeist, R., Andrä, W., Buske, N., Hergt, R., Hilger, I., Richter, U. and Kaiser, W., 1999. "Application of magnetite ferrofluids for hyperthermia". *Journal of Magnetism and Magnetic Materials*, Vol. 201, No. 1-3, pp. 420–422.

Hirsch, C., 2007. *Numerical computation of internal and external flows: The fundamentals of computational fluid dynamics*. Elsevier.

Matos, H. and Oliveira, P., 2013. "Steady and unsteady non-Newtonian inelastic flows in a planar T-junction". *International Journal of Heat and Fluid Flow*, Vol. 39, pp. 102–126.

Matos, H. and Oliveira, P., 2014. "Steady flows of constant-viscosity viscoelastic fluids in a planar T-junction". *Journal of Non-Newtonian Fluid Mechanics*, Vol. 213, pp. 15–26.

Milne-Thomson, L.M., 1996. *Theoretical hydrodynamics*. Courier Corporation.

Raj, K., Moskowitz, B. and Casciari, R., 1995. "Advances in ferrofluid technology". *Journal of Magnetism and Magnetic Materials*, Vol. 149, No. 1-2, pp. 174–180.

Rosensweig, R.E., 2013. *Ferrohydrodynamics*. Courier Corporation.

Tan, S.H. and Nguyen, N.T., 2011. "Generation and manipulation of monodispersed ferrofluid emulsions: The effect of a uniform magnetic field in flow-focusing and T-junction configurations". *Physical Review E*, Vol. 84, No. 3, p. 036317.

White, F.M., 2010. *Mecânica dos Fluidos-6a Edição*.

7. RESPONSIBILITY NOTICE

The authors are solely responsible for the printed material included in this paper.